**Atmospheric
Chemistry
and Physics**

Rayleigh lidar observation of a warm stratopause over a tropical site, Gadanki (13.5° N; 79.2° E)

V. Sivakumar[1]**, B. Morel**[1]**, H. Bencherif**[1]**, J. L. Baray**[1,2]**, S. Baldy**[1]**, A. Hauchecorne**[3]**, and P.B. Rao**[4]

[1]Laboratoire de Physique de l'Atmosphère CNRS–UMR 8105, Université de La Réunion, 15 Av. René Cassin, BP 7151, 97715 Saint-Denis Messag. Cedex 9, La Réunion, France
[2]Institut Pierre Simon Laplace (IPSL), Observatoire de Physique de l'Atmosphère de la Réunion (OPAR), La Réunion, France
[3]Service d'Aéronomie CNRS-UMR 7620, France
[4]National Remote Sensing Agency, Bala Nagar, Hyderabad – 500 037, India

Abstract. The first Rayleigh lidar observation of a stratopause warming over a tropical site, Gadanki (13.5° N; 79.2° E), is presented in this paper. The warming event was observed on 22–23 February 2001, and found to occur in the stratopause region ($\sim$45 km). The magnitude of the warming was found to be $\sim$18 K with respect to the winter-mean temperature profile derived from the lidar data collected over March 1998 to July 2001. The event observed by the lidar has also been seen in data from the Halogen Occultation Experiment (HALOE) on board the UARS satellite. The zonal-mean temperature at 80° N and the zonal-mean zonal wind at 60° N from the National Centre for Environmental Prediction (NCEP) reanalysis and the European Centre for Medium-Range Weather Forecasts (ECMWF) analysis indicate that a major warming episode took place in the northern polar hemisphere a week before the day of the observation over Gadanki. Eliassen-Palm (E-P) flux calculations from ECMWF analysis show evidence of propagation of planetary-wave activity from high and mid- to low latitudes subsequent to the major warming episode over the pole. Our results support the view that the most likely source mechanism for the observed stratopause warming is the increase in planetary-wave activity.
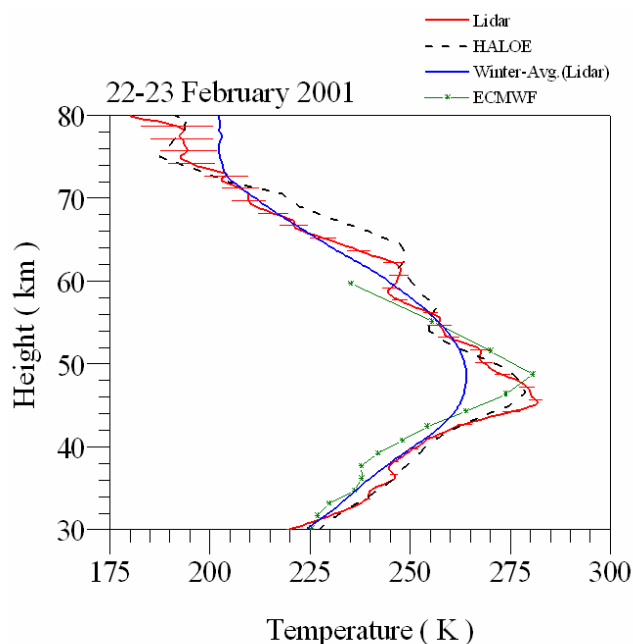
1 Introduction

One spectacular transient phenomenon observed in the middle atmosphere is the stratospheric sudden warming (SSW). Since the first observation by Scherhag (1952), many SSW's have occurred especially in the northern hemisphere. A summary of our classical understanding is provided in a review by Schoeberl (1978). He noted that sudden warmings would occur mostly in the northern polar hemisphere during win-

tertime, and that they might be associated with the anomalous growth of the planetary waves (PW) that propagate from the troposphere into the stratosphere during winter. Stratospheric warmings have been classified into major and minor warmings, depending on the amplitude of the temperature perturbations and the state of the zonal circulation (e.g. Andrews et al., 1987; Donfrancesco et al., 1996; Marenco et al., 1997). Major warmings are characterized by large perturbations of temperature, and the reversal of the zonal-mean temperature gradients along with that of the zonal-mean wind at 60° N latitude in the mid-stratosphere (at and below 10-hPa). In contrast, minor warmings are characterized by weaker perturbations of temperature, and the reversal of the zonal-mean temperature gradients only.

Schoeberl (1978) has reported that if a major warming event occurs, it usually takes 4–6 weeks for the zonal mean circulation to return to the pre-warming state. One of the well-known characteristics of a sudden warming event is the downward propagation of a warm layer from about 45 km into the lower stratosphere as seen by rocket measurements and satellite radiance data (Quiroz, 1969, 1971; Scott, 1972). The dynamical mechanisms responsible for sudden warmings involve upward propagation of planetary (Rossby) waves from the troposphere into the stratosphere where they are expected to interact with the mean flow (by breaking as they encounter a critical level). This hypothesis was first proposed by Matsuno (1971) and tested it by using a numerical model of the stratosphere. He concluded that the deceleration of the zonal wind and the concomitant temperature increase over the pole below the forcing region might account for the sudden warming phenomenon (details are also available from Shepherd, 2000). Vortex dynamics in connection to the SSW is documented by Shepherd (2000) in his review work on the middle atmosphere. He explained that if the vortex moves off the pole, then one should expect "wave-1" warming, if it splits into two, then "wave-2" warming may be expected.

Fig. 1. Lidar, HALOE and ECMWF temperature profiles for the night of 22–23 February 2001, along with the lidar mean temperature profile for winter months.

In recent years, stratospheric warmings have been observed at mid- (Hauchecorne and Chanin, 1983) and high latitudes (Whiteway and Carswell, 1994; Donfrancesco et al., 1996; Whiteway et al., 1997; Duck et al., 1998; Walterscheid et al., 2000) using lidar measurements. The cause of such warmings has been interpreted either in terms of gravity-wave (GW) activity (Whiteway and Carswell, 1994; Whiteway et al., 1997), PW activity (Hauchecorne and Chanin, 1983; Marenco et al., 1997) or formation of vortex core and PW breaking (Schoeberl, 1978; Labitzke, 1981; Duck et al., 1998; Walterscheid et al., 2000). Finally, SSW events include coolings of a few degrees in the mesosphere (Schoeberl, 1978; Appu, 1984; Delisi and Dunkerton, 1988; Duck et al., 1998; Walterscheid et al., 2000).

Besides lidar measurements, satellite and rocket measurements have also been used to report on SSW events (Appu, 1984; Dunkerton et al., 1988; Dunkerton and Delisi, 1986; Delisi and Dunkerton, 1988; Randel, 1993). Using 35 years of satellite data, Dunkerton et al. (1988) found that the occurrence of major SSW events depends on the Quasi-Biennial Oscillation (QBO) phase. In particular, they showed that major SSWs occur only when the QBO blows westerly.

Here we describe, using ground-based lidar measurements from the tropical station of Gadanki (13.5° N; 79.2° E), a warming event observed at the stratopause layer on 22–23 February 2001. The observed event is discussed in terms of PW and GW activities. To support our observation, we also present data from the Halogen Occultation Experiment

(HALOE) on board the UARS satellite. Since there have not been any reports of warmings, we believe that our result is the first of its kind as reported from a tropical station using ground-based lidar measurements.

2   Data and Analysis

The lidar data presented in this paper have been collected at the National MST Radar Facility (NMRF), Gadanki (13.8° N, 79.2° E), during the night of 22–23 February 2001 with measurements performed continuously from 20:00 to 02:00 LST. Using the photon count profiles from the lidar data and a model atmosphere (MSISE-90), temperature profiles have been derived for the height range of 30–90 km following the method of analysis given by Hauchecorne and Chanin (1980). Further details on the system and data analysis can be found in Sivakumar et al. (2001, 2003).

In addition, we use the UARS-HALOE satellite data for comparison, along with NCEP and ECMWF data to interpret the warming event.

3   Result

Lidar and satellite observations

The lidar temperature profile for the night of 22–23 February 2001 is shown in Fig. 1 (red solid line) along with the standard deviation (red horizontal bars). For comparison, the winter-monthly (Nov, Dec, Jan and Feb.) mean temperature profile derived from the lidar data collected over Gadanki from March 1998 to July 2001 (Sivakumar et al., 2003) is also displayed (blue solid line). The lidar profile for the night of 22–23 February 2001 clearly shows temperature increase in the stratopause region up to a maximum value of 283 K around 45 km. The magnitude of the warming is found to be ten times larger than the standard deviation (4 K at 70 km, 3 K at 60 km, 1–2 K at 50 km, ∼1 K at 40 km and less than 1 K at 30 km). Additionally, the HALOE temperature profile measured on the same day over the closest location (10.46° N; 73.31° E), has been included in Fig. 1 (dashed line). Agreement between lidar and satellite temperature profiles is generally good. The amplitude of the HALOE temperature maximum (281 K) during the warming event is close to that of the lidar, confirming the accuracy of the event. Small differences between the lidar and HALOE profiles exists, these are due to the poorer height resolution of the HALOE measurement (3.7 km) in comparison with that of the lidar (0.3 km) and to the observational time difference between HALOE (at sunset) and lidar (night time) measurements. The lidar observation also shows a lowering of stratopause height by 4 to 5 km with respect to the mean stratopause height (∼49 km) calculated for February months (Sivakumar et al., 2003). Finally, associated with the stratospheric warming event, the upper mesosphere region
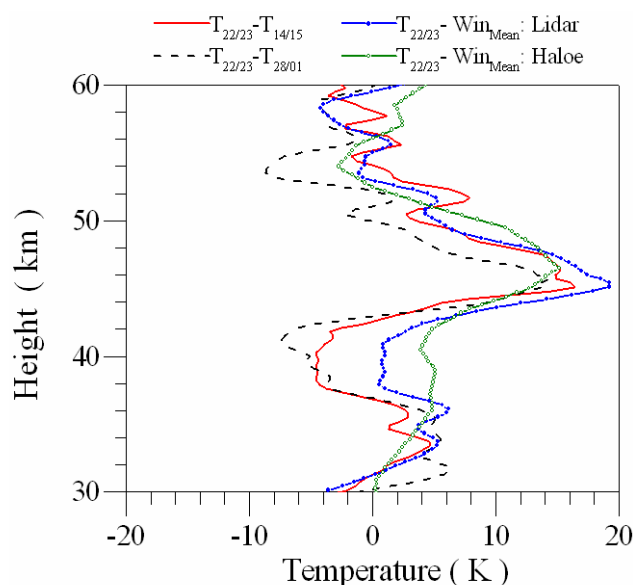
(~70–80 km), exhibits a cooling of ~10–12 K with respect to the mean profile, in accordance with results reported in other studies (e.g. Appu, 1984; Delisi and Dunkerton, 1988; Duck et al., 1998; Walterscheid et al., 2000).

Figure 2 gives estimates of the magnitude of the warming observed over Gadanki. These have been obtained by subtracting successively from the 22–23 February profile, temperature values recorded a week before (14–15 Feb.) and a week after (28 Feb.–1 March), and climatological temperature values derived from lidar and HALOE measurements. In the stratopause region, the amplitude of the warming is found to be about ~18 K with respect to the lidar-derived mean temperature profiles, and ~15–16 K for the rest of the cases. It appears that the order of magnitude of the stratopause warming observed over Gadanki is smaller than what has been reported for mid- and high latitudes in the northern hemisphere (about 30 K) (Hauchecorne and Chanin, 1983; Whiteway and Carswell, 1994; Whiteway et al., 1997; Duck et al., 1998). Moreover, both the lidar and ECMWF data present a maximum on 22–23 February 2001 as observed from the time evolution of the daily temperature values at the stratopause during the January-February-March period (figure not shown).

4 Discussion

One dynamical feature in the lidar temperature profile presented in Fig. 1 is the wave-like structure oscillating around an average profile with amplitude increasing with height. Two systems of waves are most likely responsible for this wave-like structure: planetary waves (PW) and gravity waves (GW).

GW are known to have a profound effect on the thermal and dynamical structure of the middle atmosphere. GW propagating upward from the lower atmosphere grow in response to the decreasing background atmospheric density. When they approach critical levels or when they induce convective instability, they are dissipated, and their associated momentum is deposited into the flow. This process is responsible for the phenomenon known as the mesospheric temperature inversion (Hauchecorne et al., 1987; Leblanc et al., 1995). However, Ratnam et al. (2003) reporting on mesospheric temperature inversions using 40 months of NMRF-lidar observations over Gadanki, have shown that mesospheric temperature inversions at this latitude occur in the height range of 70–80 km, with larger perturbations during summer than winter. Moreover, estimates of the GW potential energy during the lidar measurement period studied here, show an increase in GW potential energy in the stratopause region up to about 135 J kg^{-1} at the stratopause height (figure not shown). This increase is however not sufficient to explain a temperature rise of 16–18 K as that observed during the event (Sivakumar et al., 2001). In addition, a comprehensive study of the middle atmospheric
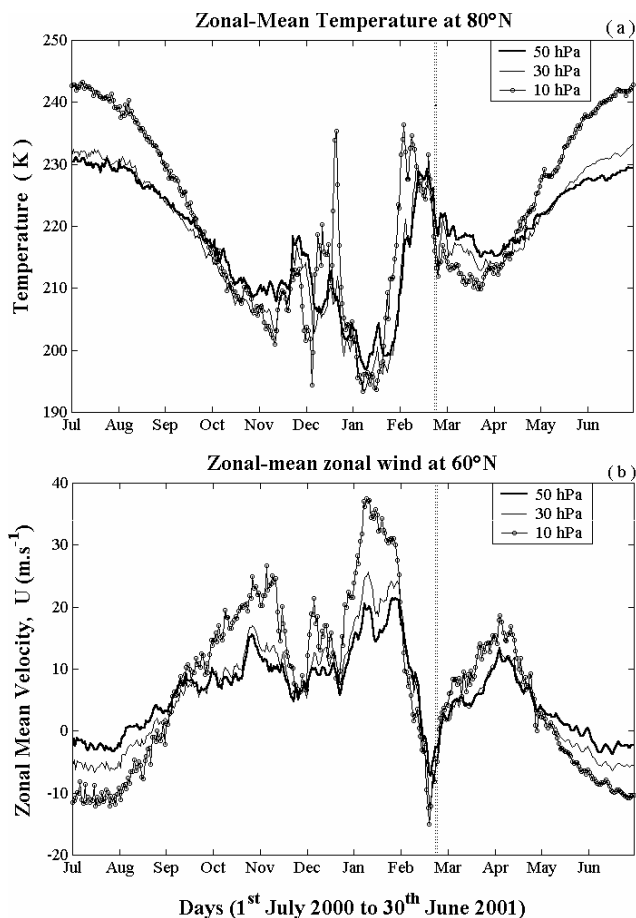

Fig. 2. Temperature differences between the 22–23 February lidar-measured temperature profile, and lidar profiles measured a week before and a week after, and lidar and HALOE winter-mean profiles. The HALOE climatological profile has been computed by compiling all the winter data recorded from 1998 to 2002, within a range of ±5° in latitude and ±10° in longitude with regards to the lidar position (13.5° N; 79.2° E).

gravity wave activity has shown the wave activity to be maximum during winter for high latitudes and during equinoctial periods for low latitudes (Fritts, 1984). Finally, Garcia and Boville (1994) have noted that the role of GW may not be as significant in the northern polar vortex as in the southern polar vortex. Thus, there should be another dynamical source, the PW activity, which may be responsible for the observed warming. This is further explored in the following sub-section.

PW drive: NCEP reanalyses and ECMWF analyses

Information about the evolution of the stratospheric state at the time of the lidar observation is provided by the NCEP and ECMWF data. NCEP and ECMWF data are used on a 2.5°×2.5° grid from 1000 to 10 hPa (15 levels) and from 1013.25 to 0.20 hPa (60 levels), respectively. As shown in Fig. 1, the stratopause-warming event can also be seen in the ECMWF data derived for the location and the date of the lidar sounding. The temperature maximum value is found to be close to that observed by the lidar, although located at a higher altitude. The altitude difference may be attributed to the poor vertical resolution of satellite radiances assimilated in ECMWF around the stratopause.

Figures 3a and b show respectively the NCEP zonal-mean temperature at 80° N and the zonal-mean zonal wind at 60° N at three different pressure levels: 50, 30 and 10 hPa, for the

Fig. 3. Variations of **(a)** the zonal-mean temperature at 80° N and **(b)** the zonal-mean zonal wind at 60° N, from 1 July 2000 through 30 June 2001 at 3 different pressure levels in the stratosphere: 50, 30 and 10 hPa, derived from NCEP data. The vertical dotted lines indicate the day of the lidar sounding.

period extending from 1 July 2000 to 30 June 2001. Examination of Fig. 3a indicates that a minor stratospheric warming occurred during the second half of January 2001 over the polar region, turning into a major warming in mid-February with the reversal of the zonal wind (Fig. 3b). The stratosphere then returned slowly to winter conditions although the circulation remained disturbed up to the beginning of March, so that the time interval for the event was approximately 45 days. It can be seen on Fig. 3, that the warming event observed in the lidar sounding over Gadanki (vertical dotted lines) appears to occur shortly after the peak of temperature and circulation anomalies over the polar region.

Planetary waves (PW) are known to be responsible for bringing about the large mean-flow changes observed during sudden warmings. To gain deeper insights into the dynamical processes occurring during the warming event of February 2001, we use isentropic maps of Ertel's potential vorticity (PV). This approach has been used elsewhere (e.g. McIn-

tyre and Palmer, 1983; Dunkerton and Delisi, 1986) to discuss the dynamics of sudden warming events in connection with breaking planetary waves (PW). In fact, using Nimbus-7 Limb Infrared Monitor of the Stratosphere (LIMS), Dunkerton and Delisi (1986) have studied the time evolution of PV in the winter stratosphere of January–February 1979, and suggested that the temporal evolution of the size, shape and orientation of the main circumpolar vortex would be revealed very clearly by the potential vorticity field. The size of the vortex determines the range of latitudes over which planetary and Rossby waves are able to propagate.
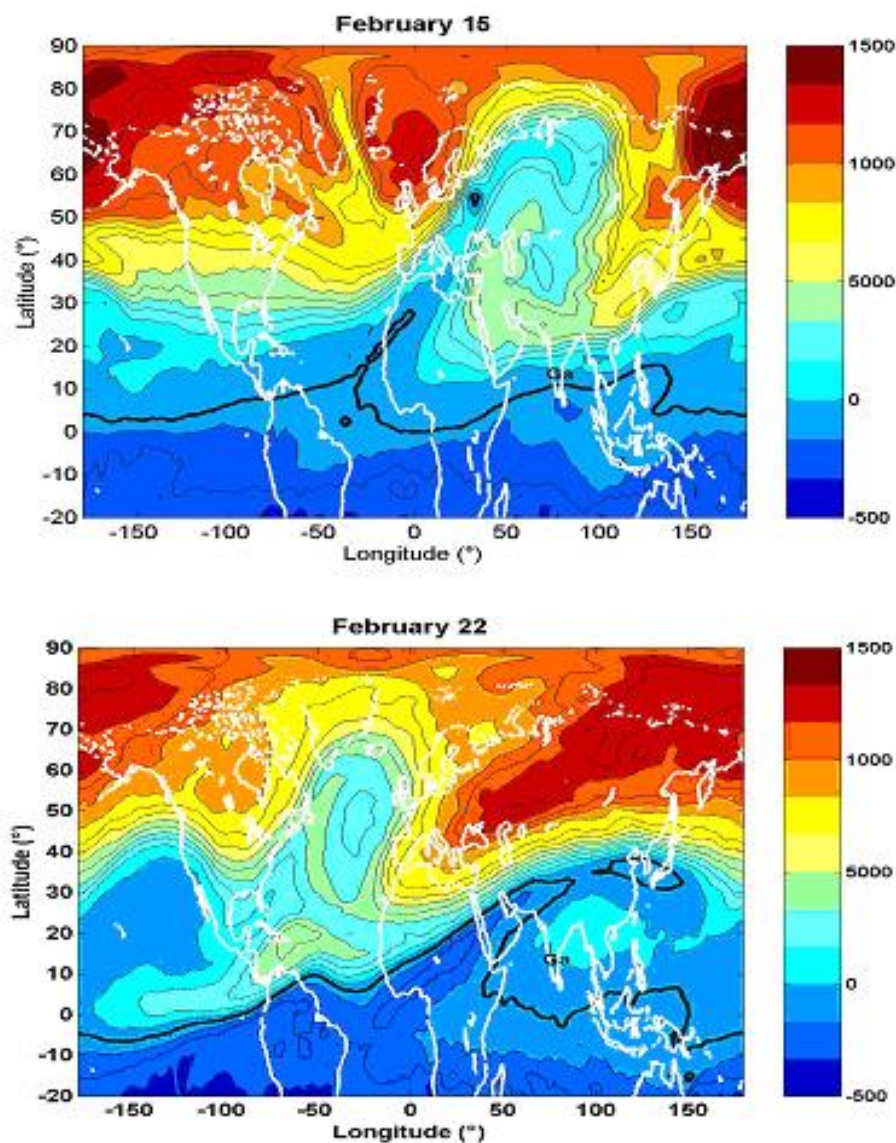
Figures 4a and b show PV maps for the 1900-K isentropic surface representing the stratopause region, calculated from the ECMWF reanalysis. The PV map obtained on 15 February, i.e. a week before the stratopause warming over Gadanki, is principally characterized by a tropical air mass (low PV) excursion northward toward the polar region, and with a longitudinal extension from 0° to 100° E (see Fig. 4a). The lidar site, indicated on the PV maps by the symbol "Ga", appears on Fig. 4a nearly under the zero-PV zone. From examination of the PV map obtained on 22 February, one can notice a "tongue" of high-PV emanating from polar latitudes and extending westward and equatorward (see Fig. 4b). Meanwhile, it is also evident from the PV-field that the air-mass "intrusion" originates from the southern tropical zone (low and negative PV) and has moved northward and eastward, with an extension up to 30° N and from ≈20° W to ≈70° E. Those PV maps thus give evidence of some horizontal exchange between the tropics and high-latitudes that has led to the formation on the 1900-K level of a large surf zone covering the lidar site, in which PV contours seem irreversibly twisted (see Fig. 4b), suggesting a process of PW drive and its breaking. Further diagnostics of the planetary-wave activity and possible breaking-wave regimes are provided by the Eliassen-Palm (EP) flux $\boldsymbol{F}$ and the divergence of the EP flux $\nabla.\boldsymbol{F}$, which are expressed in spherical geometry as:

$$\boldsymbol{F} = \left\{ f_{(\phi)}, F_{(z)} \right\} = \left\{ -\rho_0 a \cos\phi \left(\overline{v'u'} \right), f\rho_0 a \cos\phi \left(\frac{\overline{v'\theta'}}{\overline{\theta_z}} \right) \right\}$$

$$\nabla.\boldsymbol{F} = \frac{1}{a\cos\phi} \left(F_{(\phi)} \cos\phi \right)_\phi + \left(F_{(z)} \right)_z. \qquad (1)$$

Where, the overbars and primes denote zonal means and deviations there from, with all other symbols being as in Andrews et al. (1987).
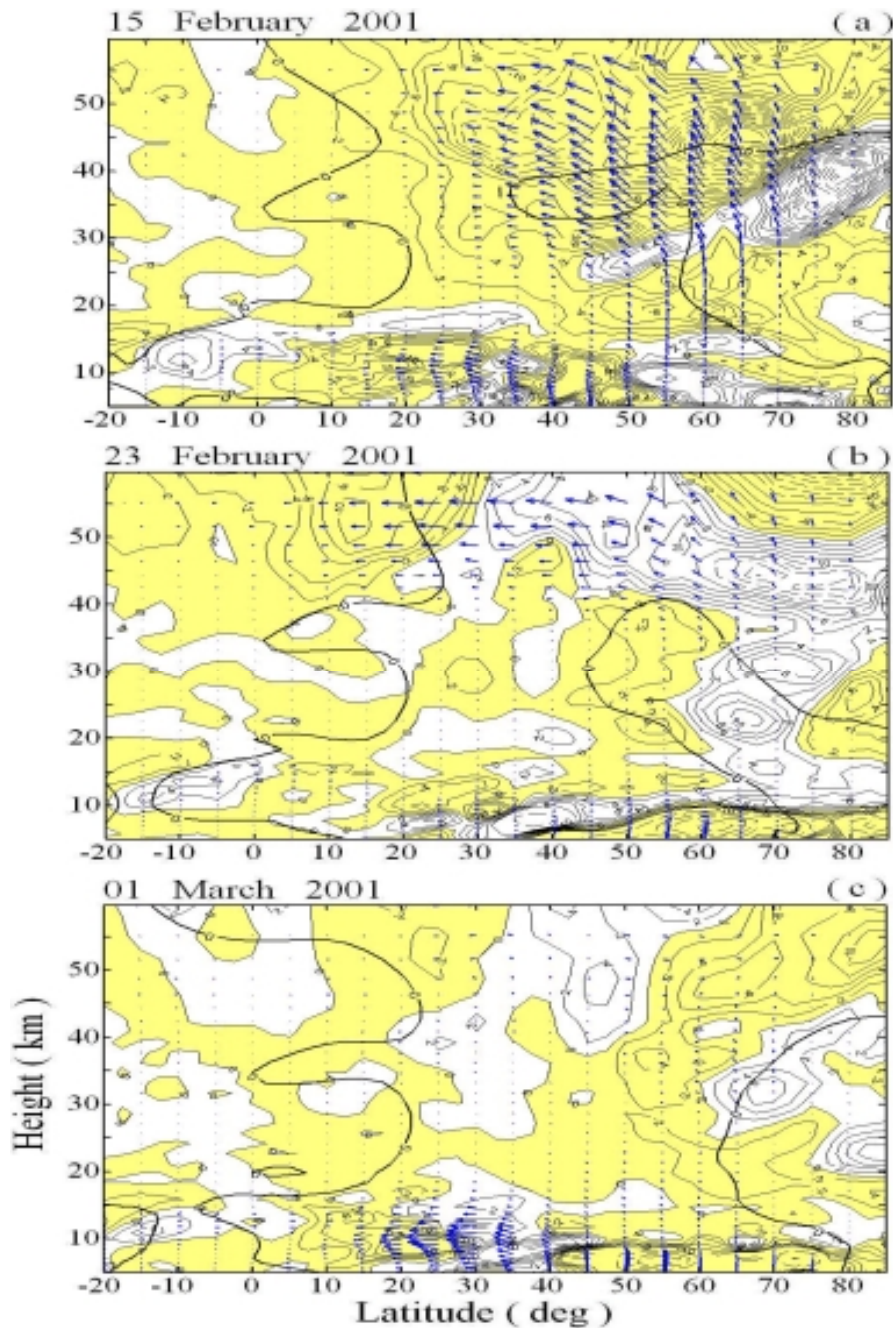
The orientation of the EP flux vector indicates the direction of PW propagation (Kanzawa, 1984; Dunkerton and Delisi, 1986; Delisi and Dunkerton, 1988). Planetary wave activity in the mid-latitudes generally propagates from the winter troposphere up into the stratosphere and toward the equator. PW breaking can be recognized by the convergence of the EP vectors ($\nabla.\boldsymbol{F} < 0$). Figures 5a, b and c are displayed latitude-altitude cross-sections of the EP flux (arrows) for several days nearby the lidar sounding. Wave fluxes in the vector's formulation are computed using ECMWF data.

Fig. 4. Evolution of Ertel's Potential Vorticity on the 1900-K isentropic surface for **(a)** 15 Feb., and **(b)** 22 Feb. 2001. The contour interval is 1×10^{-3} K kg^{-1} m^2 s^{-1} for PV$<10 \times 10^{-3}$K kg^{-1} m^2 s^{-1} (solid lines); it is 5×10^{-3} K kg^{-1} m^2 s^{-1} for PV$\geq 10 \times 10^{-3}$K kg^{-1} m^2 s^{-1} (thick solid lines). "Ga" indicates the location of the lidar station.

To allow the EP vectors to be seen clearly throughout the stratosphere, the vectors are multiplied by $e^{z/H}$ (Mechoso et al., 1985). In addition, $F_{(z)}$ is magnified by a factor 150 with respect to $F_{(\phi)}$ (Randel et al., 1987). Superimposed on these figures is the wave driving (shaded and contours) which is proportional to the EP flux divergence: $D = \frac{1}{\rho_0 a \cos \phi} \nabla \cdot \mathbf{F}$. As it can be seen from Fig. 6a, on 15 February, a week before the stratopause warming over Gadanki, strong EP flux throughout the middle atmosphere is evident over the high- and mid-latitude regions. $\mathbf{F}$ arrows indicate a vertical propagation out of the troposphere into the lower stratosphere, turning then into an equatorward propagation in the upper stratosphere and lower mesosphere region. Here the "focusing" of the waves is accompanied by large negative values of the wave driving D, on the order of several tens of meters per second per day and towards poleward of 30^{circ} latitude (dashed contours). On 23 February, the day of the stratopause warming (see Fig. 5b), the propagation is getting further equatorward into the tropical region, where the stronger wave activity and convergence of EP flux are likely to produce a rapid deceleration of the zonal-mean zonal wind (leading to the poleward migration of low-latitude easterlies – figure not shown) and the associated temperature rise. One week later (Fig. 5c), the middle atmosphere returns to normal, with planetary-wave activity remarkably weaker and confined to the high-latitude region.

Fig. 5. E-P flux cross-sections in the meridian plane for several days nearby the lidar sounding. Contours represent values of the wave driving term D (see text for definition), in m/s/day; negative wave driving is shaded. The solid and labeled contours stand for the values between -10 and 10 m/s/day with an interval of 2 m/s/day. The dashed and non-labeled contours stand for the values ≥ 12 and ≤ -12 m/s/day with an interval of 2 m/s/day for the heights above 15 km and 10 m/s/day for the heights below 15 km.

5 Conclusion and Additional Remarks

This paper reports on the first warming event observed by lidar in the stratopause region over a tropical site (Gadanki, India). The accuracy of the event was confirmed using co-located and quasi-simultaneous temperature data from HALOE on board the UARS satellite. The magnitude of the warming observed by lidar was found to be ~18 K with respect to the winter monthly-mean temperature profiles derived from the lidar/HALOE data collected over March 1998 to July 2001. This is less than what is usually reported over mid- and high-latitude regions in the northern hemisphere

(about 30 K) (Hauchecorne and Chanin, 1983; Whiteway and Carswell, 1994; Whiteway et al., 1997; Duck et al., 1998). The warming event over Gadanki appeared to occur about a week after a major stratospheric warming event over the polar region. Using EP flux calculations from ECMWF analyses, we found that the event was mainly driven by PW propagating from high and mid- to low latitudes consecutive to the major warming episode over the pole. Though the temperature perturbation during the event was too large to be due only to GW, it is suspected that enhancement in GW activities through interactions with PW and mean flow may have large impacts on the temperature profile. Since the objective of the paper was to report on the observed event, the expectation of a quadrupole moment between the poles and the tropics (Delisi and Dunkerton, 1988) has not been explored here. In future, the above issues will be addressed through coupling experimental data with model simulations and quantification tools.

Edited by: W. Ward

References

Andrews, D. G., Holton, J.R,. and Leovy, C. B.: Middle Atmosphere Dynamics, Acad. Press, 1987.

Appu, K. S.: On Perturbations in the Thermal structure of Tropical stratosphere and Mesosphere in Winter, Indian Journal of Radio and Space Physics, 13, 35–41, 1984.

Delisi, D. P. and Dunkerton, T. J.: Seasonal variation of the semi-annual oscillation, J. Atmos. Sci., 45, 2772–2787, 1988.

Donfrancesco, G. D., Adriani, A., Gobbi, G. P., and Congeduti, F.: Lidar observations of stratospheric temperature above McMurdo Station, Antartica, J. Atmos. Terr. Phys., 58, 1391–1399, 1996.

Duck, T. J., Whiteway, J. A, and Carswell, A. I.: Lidar observations of gravity wave activity and arctic stratospheric vortex core warming, Geophys. Res. Lett., 25, 2813–2816, 1998.

Dunkerton, T. J. and Delisi, D. P.: Evolution of potential Vorticity in the winter stratosphere of January–February 1979, J. Geophys. Res., 91, 1199–1208, 1986.

Dunkerton, T. J., Delisi, D. P., and Baldwin, M. P.: Distribution of Major Stratospheric warmings in relation to the Quasi-Biennial Oscillation, Geophys. Res. Lett., 15, 136–139, 1988.

Fritts, D. C.: Gravity wave saturation in the middle atmosphere: A review of theory and observations, Rev. Geophys. Space Phys., 22, 275–308, 1984.

Garcia, R. R. and Boville, B. A.: "Downward Control" of the mean meridional circulation and temperature distribution of the polar winter stratosphere, J. Atmos. Sci., 51, 2238–2245, 1994.

Hauchecorne, A. and Chanin, M. L.: Density and temperature profiles obtained by lidar between 35 and 70 km, Geophys. Res. Lett., 8, 565–568, 1980.

Hauchecorne, A. and Chanin, M. L.: Mid latitude observations of planetary waves in the middle atmosphere during the winter over 1981–1982, J. Geophys. Res., 88, 3843–3849, 1983.

Hauchecorne, A., Chanin, M. L, and Wilson, R.: Mesospheric temperature inversion and gravity wave breaking, Geophys. Res. Lett., 14, 933–936, 1987.

Kanzawa, H.: Four observed sudden stratospheric warmings diagnosed by the Eliassen-Palm flux and refractive index, Dynamics of the Middle Atmosphere, in: Proceedings of a U.S.-Japan Seminar, Honolulu, Hawaii, 8–12 November, 1982, edited by Holton, J. R. and Matsuno, T., p. 307–331, 1984.

Labitzke, K.: Stratospheric-mesospheric midwinter disturbances: a summary of observed characteristics, J. Geophys. Res., 86, 9665–9678, 1981.

Leblanc, T., Hauchecorne, A., Chanin, M. L., Taylor, F. W., Rodgers, C. D., and Livesey, N.: Mesospheric temperature inversions as seen by ISAMS (UARS), Geophys. Res. Lett., 22, 1485–1488, 1995.

Marenco, F., di Sarra, A., Cacciani, M., Fiocco, G, and Fua, D.: Thermal structure of the winter middle atmosphere observed by lidar at Thule, Greenland, during 1993–1994, J. Atmos. Solar. Terr. Phys., 59, 151–158, 1997.

Matsuno, T.: A dynamical model of the stratospheric sudden warming, J. Atmos. Sci., 28, 1479–1494, 1971.

McIntyre, M. E. and Palmer, T. N.: Breaking planetary waves in the stratosphere, Nature, 305, 593–600, 1983.

Mechoso, C. R., Hartmann, D. L., and Farrara, J. D.: Climatology and interannual variability of wave, mean-flow interaction in the Southern Hemisphere, J. Atmos. Sci., 42, 2189–2206, 1985.

Quiroz, R. S.: The warming of the upper stratosphere in February 1966 and the associated structure of the mesosphere, Mon. Weather. Rev., 97, 541–552, 1969.

Quiroz, R. S.: The determination of the amplitude and altitude of stratospheric warmings from satellite measured radiance changes, J. Appl. Meterol., 10, 555–574, 1971.

Randel, W. J., Stevens, D. E., and Stanford, J. L.: A study of planetary waves in the southern winter troposphere and stratosphere, Part II: Life cycles, J. Atmos. Sci., 44, 936–949, 1987.

Randel, W. J.: Global variations of zonal mean ozone during stratospheric warming events, J. Atmos. Sci., 50, 3308–3321, 1993.

Ratnam, M. V., Nee, J. B., Chen, W. N., Sivakumar, V., and Rao, P. B.: Recent observations of mesospheric temperature inversions over a tropical station (13.5° N; 79.2° E), J. Atmos. Solar Terr. Phys., 65, 323–334, 2003.

Scherhag, R.: Die explosionsartige Stratosphärenerwärmung des Spätwinters 1951/52, Ber. Deut. Wetterdienst, 38, 51–63, 1952.

Schoeberl, M. R.: Stratospheric warmings: observations and theory, Rev. Geophys. Space Phys., 16, 521–538, 1978.

Scott, A. F. D.: Mesospheric temperatures and winds during a stratospheric warming, Phil. Trans.Roy. Soc. London, 271, 547–557, 1972.

Shepherd, T. G.: The middle atmosphere, J. Atmos. Solar. Terr. Phys., 62, 187–1601, 2000.

Sivakumar, V., Bhavanikumar, Y., Raghunath, K., Rao, P. B., Krishnaiah, M., Mizutani, K., Aoki, T., Yasui, M., and Itabe, T.: Lidar measurements of mesospheric temperature inversion at a low latitude, Ann. Geophys., 19, 1039–1044, 2001, **SRef-ID: 1432-0576/ag/2001-19-1039**.

Sivakumar, V., Rao, P. B., and Krishnaiah, M.: Lidar measurements of stratosphere-mesosphere thermal structure over a low latitude: Comparison with satellite data and models, J. Geophys. Res., 108, D11, 4342,10.1029/2002JD00 3029, 2003.

Walterschied, R. A., Sivjee, G. G., and Roble, R. G.: Mesospheric and lower thermosphere manifestations of a stratospheric warming event over Eureka, Canada (80° N), Geophys. Res. Lett., 27, 2897–2900, 2000.

Whiteway, J. A. and Carswell, A. I.: Rayleigh lidar observations of thermal structure and gravity wave activity in the high arctic during a stratospheric warming, J. Atmos. Sci., 51, 3122–3136, 1994.

Whiteway, J. A. Duck, T. J., Donovan, D. P., Bird, J. C., Pal, S. R., and Carswell, A. I.: Measurements of gravity wave activity within and around the Arctic stratospheric vortex, Geophys. Res. Lett., 24, 1387–1390, 1997.